

# RSC Advances



This is an *Accepted Manuscript*, which has been through the Royal Society of Chemistry peer review process and has been accepted for publication.

*Accepted Manuscripts* are published online shortly after acceptance, before technical editing, formatting and proof reading. Using this free service, authors can make their results available to the community, in citable form, before we publish the edited article. This *Accepted Manuscript* will be replaced by the edited, formatted and paginated article as soon as this is available.

You can find more information about *Accepted Manuscripts* in the [Information for Authors](#).

Please note that technical editing may introduce minor changes to the text and/or graphics, which may alter content. The journal's standard [Terms & Conditions](#) and the [Ethical guidelines](#) still apply. In no event shall the Royal Society of Chemistry be held responsible for any errors or omissions in this *Accepted Manuscript* or any consequences arising from the use of any information it contains.

## Title Page:

## Original Research Article

## Article title:

**Cellular uptake, imaging and pathotoxicological studies of Novel Gd [III]-DO3A-butrol Nano-Formulation**

*Elham Mohammadi,<sup>1</sup> Massoud Amanlou<sup>2</sup>, Seyed Esmaeil Sadat Ebrahimi<sup>2</sup>, Morteza Piralı Hamedani<sup>2</sup>, Abdolkarim Mahrooz<sup>3</sup>, Bitā Mehravi<sup>4</sup>, Baharak Abd Emami<sup>5</sup>, Mohammad Reza Aghasadeghi<sup>6</sup>, Ahmad Bitarafan-Rajabi<sup>7</sup>, Hamid Reza Pour Ali Akbar<sup>8</sup>, Mehdi Shafiee Ardestani<sup>9\*</sup>,*

*1-Department of biochemistry, Faculty of Biochemistry, Mazandaran University of Medical Sciences, Mazandaran Iran*

*2- Department of Medicinal Chemistry, Faculty of Pharmacy, Tehran University of Medical Sciences, Tehran, Iran*

*3- Molecular and Cell Biology Research Center, Mazandaran University of Medical Sciences, Sari, Iran*

*4- Faculty of Advanced Technologies in Medicine, Iran University of Medical Sciences, Tehran, Iran*

*5-National Cell Bank, Pasteur institute of Iran, Tehran, Iran*

*6-Department of Hepatitis and AIDS, Pasteur Institute of Iran, Tehran, Iran*

*7-Cardiovascular interventional research Centre; Department of Nuclear Medicine, Rajaei Cardiovascular, Medical & Research Center; Iran University of Medical Sciences, Tehran, Iran*

*8-Cardiovascular, Medical & Research Center; Radiology Department; Iran University of Medical Sciences, Tehran, Iran*

*9- Department of Radiopharmacy, Faculty of Pharmacy, Tehran University of Medical Sciences, Tehran, Iran*

**Running title (Novelty):** Cellular uptake and imaging studies of Novel Gadobutrol-ALGD-G2

*\*Address correspondence to this author at the Department of Radiopharmacy, Faculty of Pharmacy, Tehran University of Medical Sciences, Tehran, Iran, Tel/Fax: +98-021-66953311*

E-mail: [shafieeardestani@gmail.com](mailto:shafieeardestani@gmail.com), [shafieeardestani@sina.tums.ac.ir](mailto:shafieeardestani@sina.tums.ac.ir)

**Table of contents:**

**1-Graphical Abstract**

**2-Abstract**

**3-Introduction**

**4-Results and Discussion**

**4-1 Size and zeta potential distribution**

**4-2 Apoptosis assay**

**4-3 Intra-cellular uptake of GALGD into tumor cells**

**4-4 Relaxation**

**4-5 Tumor Imaging**

**4-6 Pathological Findings**

**4-7 Protein Corona**

**5- Chemical Experimental**

**5-1 Instrumentation**

**5-2 Animals**

**5-3 GALGD-G2 Synthesis and Gadobutrol-GALGD-G2 nano-formulations**

**5-4 Cell culture**

**5-5 Apoptosis-Necrosis assay**

**5-6 Nano-formulation intra-cellular uptakes**

**5-7 Evaluation of Protein Corona**

**6- MR measurement and Stability Studies**

**6-1 *In vivo* MRI preparation**

**7- Pathological Findings**

**8- Statistical Analysis**

**9- CONCLUSION**

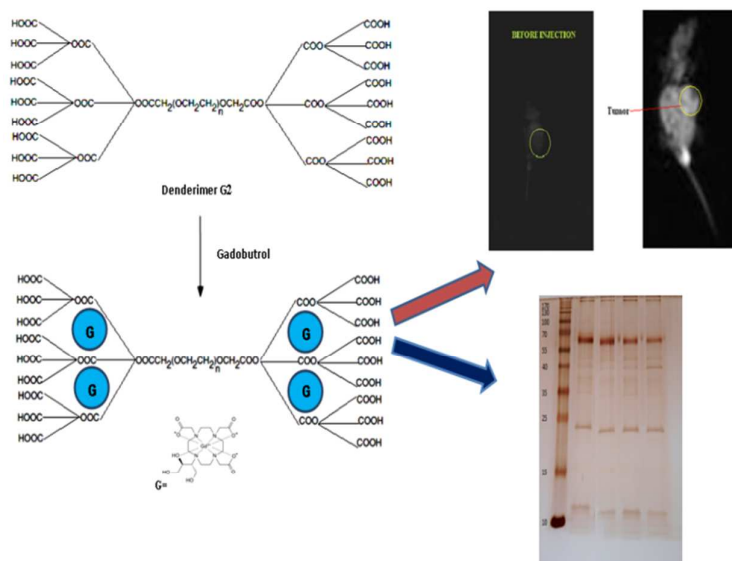
**10-ACKNOWLEDGEMENTS**

**11-Disclosure**

**12-Bibliographic references and notes**

## Graphical Abstract:

## Cellular uptake, imaging and pathotoxicological studies of Novel Gd [III]-DO3A-butrol Nano-Formulation



## Abstract

The high adaptability of dendrimer-based contrast agents is ideal for the reliable molecular imaging of cancerous tissues. Gadobutrol [ $\text{Gd}^{3+}$  [III]-DO3A-butrol, gadovist] is one of the contrast media which is produced commercially and used clinically. In this study, the gadobutrol was nano-formulated by adding different ratios [X, 2X] of Anionic Linear Globular Dendrimer G2 [Gadobutrol-ALGD-G2 nano formulation] to evaluate its intracellular uptake, pathotoxicological and molecular in vitro and in vivo imaging in cancer cells. Drug stability studies were carried out to ensure the proper formulation, after which the percentage of the drug entry as well as the levels of cytotoxicity [HEK cell line, KB cell line] were evaluated into the cancer cells [KB cell line]. The intracellular uptake Gadobutrol-ALGD-G2 was measured quantitatively with the spectroscopy of inductively coupled plasma atomic emission. The relaxometry of this contrast agent and the tumor imaging was determined using a 1.5 Tesla MRI. Results indicated that the cellular uptake of Gadobutrol-ALGD-G2 was about 71%. The  $r_1$  relaxation of this contrast agent was measured to be  $4.75 \text{ mM}^{-1} \text{ s}^{-1}$  and on a per gadolinium [ $\text{Gd}^{3+}$ ] basis. In addition, the nano-formulated Gd [III]-DO3A-butrol was able to enter the KB cancer cells. It should be noted that the apoptosis assay and the pathological evidences verified that the cells did not show significant toxicity on drug exposure, and the MRI use is feasible for quantitative evaluation of delivery and detection of cancer cells. Obtained results suggest that Gadobutrol-ALGD-G2 new nano-formulation provided a guideline in selecting these contrast agents as an appropriate contrast agent for medical nanotechnology applications.

*Keywords:* cellular uptake, contrast agent, Dendrimer, molecular imaging, MRI

---

## 1- Introduction

Cancer is defined as the uncontrolled growth of unusual cells in the human or animal body. Despite the efforts made for prevention, diagnosis and treatment of cancer, still this disease is one of the most significant reasons of morbidity across the world. <sup>1</sup> Metastatic phenomenon is the most commonly reasons for the unsuccessful cancer therapy. Additionally, this is well understood that different types of cancer usually do not show any clinical symptoms in early stages. <sup>2</sup>

Early tumor diagnosis or detection is one of the significant key factors for treatment of such malignancies. Nowadays, reports on cancer therapy demonstrated that numerous methods of traditional tumor treatment were greatly unsuccessful with very low good prognosis because of many reasons such as high cost, drug side effects and late diagnosis. Different ways of treatment are costly and not friendly for patients, so perhaps the best way of cancer treatment is limited to early detection by non-invasive techniques including molecular imaging modalities. <sup>3,4</sup>

Among different diagnostic methods, many pharmaceuticals have been discovered as molecular imaging and as a safe effective approach for early stage cancer imaging.<sup>3</sup> The Magnetic Resonance Imaging (MRI) is one of the most useful molecular imaging methods. MRI is a noninvasive imaging method for pathological diagnosis (such tumor) at an early stage. Imaging of the hydrogen nucleus is the base of MRI method in the water tissue. Water content and relaxation ratios of protons are different between in tumor tissue and surrounding normal tissues as well.<sup>1, 5-7</sup>

Contrast agents (CA) have also been most commonly used in MRI for detection and diagnostic imaging such as tumor. Currently,  $Gd^{3+}$  [III]-based MRI CA are routinely used for improving diagnostic imaging.  $Gd^{3+}$ -DTPA-dimeglumine [Magnevist<sup>®</sup>] was the first MRI approved CA for clinical use in 1988.<sup>8-10</sup>

Low specificity, cellular uptake and providing the enough relaxation to the cancer tissues of CA, due to its extracellular distribution are the main barriers to obtain the suitable specific molecular contrast agent, so it is essential to design tumor targeting MRI CA, because it is actively presuming. Currently, there are being many increased the literatures reported designing and evaluation of novel molecular specific membrane's permeability MRI contrast agents.<sup>2, 11-18</sup>

New developments in the molecular imaging objectives have been prompted during recent years. One of these approaches includes the synthesis of covalently or no covalently bound macromolecular nanoparticle based gadolinium [III] ions chelates such as dendrimers.<sup>3,7,19</sup> Previous studies on the impact of Gadolinium in MRI have shown that the gadolinium indicates the largest decrease in relaxation time [T1] and in the T2 between the compounds among other lanthanide paramagnetic available metal ions such as iron, copper and manganese.<sup>8</sup> The Compounds containing gadolinium are considered as one of the best contrast agents in MRI.  $Gd^{3+}$ -DOTA [Gadovist,  $Gd$  [III]-DO3A-butrol, gadobutrol] as macro cyclic chelate has high thermodynamic and kinetic stability as compared with those of linear chelates like  $Gd^{3+}$ -DTPA [Magnevist] which has been rapidly eliminated from the body after administration.<sup>20, 21</sup>

Major limitations in clinical applications of Small molecular  $Gd$ [III] chelates is relatively a low relaxation but Macromolecular  $Gd$ [III] complexes improve pharmacokinetics and relaxation of  $Gd$ [III]-based agents. In addition, the Macromolecular  $Gd$ [III] complexes enjoy a long blood circulation and accumulate in tumor tissues by the EPR effect, so it can provide long time span for imaging and showing no significant pathotoxicological effects like magnevist or gadovist.<sup>22, 23</sup>

Enhancing relaxation of the  $Gd$  [III] based contrast agents were observed by  $Gd$  [III] chelates attachment to macromolecules such as nano-polymeric structures. Currently diverse chemically designed dendrimers have been increasingly used as the best candidate for the delivery of contrast agents in molecular imaging as compared with other

nanoparticles due to their biocompatibility and biodegradability properties. In addition, because of their controllable properties such as water solubility, drug loading ability, monodispersity and large numbers of function able for bio-conjugation, dendrimers are of high interesting choice of drug delivery purpose.<sup>3, 7, 24-27</sup>

Towards improving the molecular paramagnetic MR contrast agents many researchers have demonstrated that chemically designed dendrimers are talent macromolecular structures to load or even conjugate to multiple  $Gd^{3+}$  based chelates.<sup>11-16</sup> Such highly branched chemically designated nanomaterials have a partial molecular weight and with a definitely identified amounts of terminal groups, that reside in their identical characteristics.<sup>17,18</sup> The scientists depicted the conjugation of  $Gd^{3+}$ -DTPA molecules to diverse generations of poly (amidoamine) (PAMAM) and poly(propylene imine) (PPI) dendrimers, by incorporation of isothiocyanate-activated p-nitrophenylalanine-based DTPA chelates. Such dendritic magnetic resonance molecular imaging agents were found to be rather beneficial for *in vivo* molecular angiography, molecular lymphography, assay of molecular imaging contrast radiopharmaceuticals distribution or clearance and target specific imaging.<sup>16,19-22</sup> Additionally, it was clearly stated that the  $r_1$  relaxivity value significantly enhances almost linearly incorrelation with molecular weight of the chemically designed dendrimer based molecular contrast agent accomplished as conjugate or loaded by diethylene triamine penta acetic acid DTPA as  $Gd^{3+}$  chelating agent.<sup>16</sup>

Furthermore, High toxicity, difficulties in the synthesis pathway and high production cost of first generation dendrimers like PAMAM, PPI and etc, are one of the most important limitations in their specifications. To improve the problems, two important strategies were employed, biodegradable core (poly ethylene glycol PEG, low price and available) first and secondly surface engineering [for instance, acetic acid modification considering the facile and one pot synthetic pathway], in this research PEG is used as the biodegradable, low price good available core, in addition, citric acids were applied as surrounding group (to produce an anionic linear globular dendrimer, ALGD) which it has been well known that both molecules were completely metabolized safely in the human body. In addition, the reports indicated that PEG can be significantly accumulated in cancerous tissues without any targeting agent while citric acids surface provides solubility of such negatively charged dendrimer. The negative charge of citric acid groups in surrounding dendrimer prevents interaction with cell surface and this charge property does not cause the damage of cell membrane and subsequent pathotoxicological effects. In addition, the citric acid is quickly metabolized in body, so it is biodegradable and nontoxic. As a result, probably such dendrimer is recognized as biodegradable and biocompatible nano-polymer with no significant toxicity.<sup>3, 28, 29</sup>

In this study, for the first the  $Gd$  [III]-DO3A-butrol, formally known as the gadobutrol was nanoformulated based on Anionic Linear Globular Dendrimer G2 [GALGD] as well as its physico chemical properties, cellular uptake, imaging and pathotoxicological studies were also investigated *in vitro* and *in vivo* as a novel MR molecular tumor contrast agent. It should be noted that DTPA is an *in vivo* unstable metal chelator than DOTA which incorporated in gadobutrol chemical structure. As a result, such nano-formulations would be more desirable that those one cited in the literature.<sup>16-20</sup>

## 2- Results and Discussion

### 2-1 Size and zeta potential distribution

Table 1 illustrates the reduction zeta potential for Gadobutrol drug after binding to dendrimers due to the existence of negative groups on the dendrimer surface. Zeta size reported 90 nm for alone dendrimer-G2 Size and 169.4 and 525.5 nm for nano-formulation size [G+XD, G+2XD] respectively [fig5]. The same confirming evidence was obtained by performance of AFM and SEM imaging (See supplementary materials) which showed a rough sphere particles (SEM after sonification) and larger particles in AFM (Without any sonification) which indicated the inherent avidity of nanoparticles to make an aggregate.

### 2-2 Apoptosis assay

Apoptosis is a cell death mode that occurs under normal physiological conditions and the cell is an active participant in its own demise. Our findings don't demonstrate statistically significant responses in apoptotic cell to GALGD-G2s [G+XD, G+2XD] compared with Gadobutrol [Fig.2]. Apoptotic and/or necrotic cells were determined by employing Annexin V-PI Staining Kit [PI: Propodeum Iodide] based on the protocols cited in the Kit's manual. Fig.3 illustrates the percentage of apoptotic cell in flow Cytometry. The same confirming evidence was observed by performance of MTT cellular assay (See supplementary materials)

### 2-3 Intra-cellular uptake of GALGD into tumor cells

The affinity of tumor cells to the GALGD-G2 is shown in Fig.4. The ICP-AES results have showed the cell entering level for GALGD-G2 into two concentrations of [Gad+XD, Gad+2xD] rather than, the Gadobutrol is significantly increased.

### 2-4 Relaxation

The MRI relaxation times were measured for GALGD-G2, using a 1.5 Tesla MRI scanner. The GALGD-G2 showed large longitudinal [r1] and transverse [r2] relaxations. The r1 and r2 values were 4.57 mM<sup>-1</sup>s<sup>-1</sup> and 10.18 mM<sup>-1</sup>s<sup>-1</sup>, respectively while the r2:r1 ratio was 2.3 [Fig.6].

### 2-5 Tumor Imaging

A MRI study was carried out on animal models to evaluate the in vivo capability of the Gadobutrol-GALGD-G2 nanoformulation and discriminate between tumor and normal tissues. Results indicated that the tumor images were obtained a few minutes after the injection and the amount of internalized GALGD-G2 was large enough to yield a significant

effect on the MRI signal intensity [Fig. 7] and as you can see in figure 8, the tumor is clearly visible after injecting the Gadobutrol-GALGD-G2 nanoformulation.[Fig.8]

## 2-6 Pathological Findings

As could be seen easily in Fig. 9, no significant pathological defects were observed in normal and treated animals.

## 2-7 Protein Corona

It has been shown that the interaction between NPs and physiological fluids leads to the formation of protein corona onto the surface of Dendrimer based gadobutrol.<sup>32-34</sup> The type and amount of the associated proteins at the surface of nanoparticles could define their biological fate. According to the achieved results [SDS-PAGE], one can find that the protein profile of the nano-objects did not change the protein profile [See Fig 10].

In this study, anionic linear globular dendrimer-ALGD was used as a nanocarrier and relaxation enhancing agent for Gd [III]-DO3A-butrol contrast as a low cost available and safe nanoparticle considering the facile and easy synthetic pathway. The development of novel CAs that relatively or specifically accumulates at the cancerous targets is critical for cancer cell imaging, specifically in the MRI. Nanoformulation of Gd [III]-DO3A-butrol on dendrimer can be used to increase the specific accumulation of these nanocarriers within the target cancerous tissue by increasing the intracellular uptake ability and tumor kinetically attraction of poly ethylene glycol moiety.

Recent studies attempted to design novel synthesis strategies to reduce the toxicity of the dendrimers.<sup>35</sup> In current experiment the PEG is used as the biodegradable core and citric acids are applied as surrounding groups. The PEG showed to be accumulated in cancerous tissue without manipulation of any targeting agent and its core provides solubility of dendrimer.<sup>35</sup>

Moreover, Gd<sup>3+</sup> ion release from the chelator may cause severe kidney toxicological features in the body.<sup>30-35</sup> The previously reported nanoformulations oftenly used DTPA as a chelator and it has definitely shown that DTPA *in vivo* stability as linear class of chelators is significantly lower than other one class of chelators called macrocyclics like DOTA which employed in the current experiments. As a result, the current proposed nanofurmulation will formed a more stable complex than DTPA chelates.

Its negative charge's surrounding the citric acid groups caused to evade any interaction with cell membrane and subsequently cellular damage. In addition, the citric acid is quickly metabolized by the body, so it is biodegradable and not toxic.<sup>3, 7, 19, 29</sup>

In the present study, the intracellular uptake of Gd [III]-DO3A-butrol-GALGD-G2 nanoformulation was respectively assessed by ICP-AES. The intracellular uptake of Gadobutrol-GALGD-G2 nanoformulation was also studied based on transverse *in vitro*

relaxations [r1], with increasing concentration of labeled cells dispersed in homogenous phantoms. The in vitro studies on human cancer cell line showed that the Gadobutrol-GALGD-G2 nanoformulation is taken up by cells two to seven times more efficiently than that of Gd [III]-DO3A-butrol. On the other hand, such nano-formulation also leads to a significant Gd3+ ions cellular uptake to cancerous cells.

ALGD nano-polymer has numerous pores for drug loading such as Gd[III]-DO3A-butrol. The loading ability might be potentially increased by adding more groups of citric acid and increasing the generation of dendrimer<sup>36</sup>, so ALGD second generation G2 was chosen as the nano-formulation base.

Gadobutrol standard drug is an extracellular contrast media and has no ability to entering the cells. But, according to the results by Gd[III]-DO3A-butrol loading into dendrimer, the drug significantly entered into the cancerous cells. Receptor-mediated endocytosis is a proposed mechanism of dendrimers entry into cells, after entering cell, goes lysosomes for cellular digestion.<sup>25, 30-36</sup>

The ICP-AES results showed that the intracellular uptake of Gadobutrol-GALGD-G2 nanoformulation into cancerous cells was on average of  $4.4 \times 10^{-3}$  pg Gd3+ per cell, which was correlated with other studies that used the serine-derivated carbon nanotube to label the KB cell line 15, Gd3+-based single-wall carbon nanotube in a mouse macrophage cell line 37 and glucosylated Gd3+- based meso-porous silica nano-spheres.<sup>15</sup>

Biocompatibility<sup>25-30</sup> is a major concern when Gadobutrol-GALGD-G2 nanoformulation is introduced into cells. After cells treated with Gadobutrol-GALGD-G2 nanoformulation, the results showed no significant changes in the normal cells viability compared to control group. The results including apoptosis assay and MTT assay data (See supplementary materials) are in confirmation with previous studies.<sup>15, 18</sup>

Additionally, the relaxation data of Gadobutrol-GALGD-G2 nanoformulation designed as novel molecular MR contrast agent are of essential importance. The r1 and r2 values were found 4.57 and 10.18 mM<sup>-1</sup>s<sup>-1</sup> in phantom, respectively and the r2:r1 ratio was 2.3. This result showed that Gadobutrol-GALGD-G2 nanoformulation is a good T1 weighted contrast agent. We attributed the increased MR Relaxation to accessibility of water molecules at Gd3+. The T1-weighted image enhancements were also related to T1 relaxation times reduction. Recent reports used GD-ALGD2-C595 as a CA in breast cancer.<sup>15</sup> Their result showed potential GD-ALGD2-C595 in selective and molecular targeting of the breast tumor cells.<sup>7, 19</sup>

In conclusion, Gd [III]-DO3A-butrol nanoformulation has shown a more significant relaxation or cellular uptake than alone Gd [III]-DO3A-butrol and in comparison with other similar gadolinium based CAs cited in the literature such as gadopentatedimeglumine, Gadodiamide or even comparable data than their nano-conjugates considering the same analytical methods.<sup>3, 38</sup> It must be noted that some studies reported the higher relaxivity

values for dendrimeric based nanoconjugates as newer molecular imaging agents than Gd [III]-DO3A-butrol nanoformulation but there is not a good reason to make a significant difference between Gd [III]-DO3A-butrol nanoformulation and other proposed contrast agents like Gd<sup>3+</sup>-DTPA-PAMAM or PPI nanoconjugates<sup>16</sup> because first, the employed apparatus (HNMR or Relaxometer) in those experiments is different from the current experiment (MRI) and second Gd<sup>3+</sup>-DTPA conjugated to chemical structure of dendrimers whereas we loaded gadobutrol on the dendrimer. Additionally, MRI relaxivity data (which is near to clinical use of MRI radiopharmaceutical) usually obtained at higher level than HNMR or relaxometers and as a result such data have not the same nature and are not comparable at all. Furthermore, previous studies used DTPA as radio-metal-chelator which its *in vivo* stability is significantly lower than other one DOTA which employed in current experiments. Lower price, facile and easy synthetic pathway, convincing biocompatibility and biodegradability of anionic linear globular dendrimer-G2 makes it as a very promising chemically designated dendrimer for the future use in the clinic practice and manufacturing of such contrast imaging agents as well. The effectiveness of Gadobutrol-GALGD-G2 nanoformulation was elaborately evaluated as done *in vivo* MR contrast agent. Result has shown the ability of Gadobutrol-GALGD-G2 nanoformulation in enhancing the T1-weighted images. It demonstrated the efficacy of Gadobutrol-GALGD-G2 nanoformulation as shown by T1 contrast agents *in vivo*. The tumor images took a few minutes after tail vein injection (0.2 mL/B.W) of Gadobutrol-GALGD-G2 nanoformulation and alone Gd[III]-DO3A-butrol injection, indicating the utility of Gd[III]-DO3A-butrol -GALGD-G2 nanoformulation as a potential tumor and gastrointestinal MRI contrast agent.

### 3- Chemical Experimental

Fetal bovine serum [FBS], penicillin, streptomycin, and Phosphate-buffered saline [powder, pH 7.4], adipic acid dihydrazide [ $\geq 98\%$ ] were purchased from Sigma Aldrich Co. [USA], Anhydrous ethanol [EtOH, 99.5%], anhydrous N, N -dimethyl formamide [DMF, 99.8%] were provided by Acros Co. [Belgium]. Dialysis bag with 500 Da cut off was obtained from the Spectrum Lab. [USA]. Gadovist® [gadobutrol] was obtained from Bayer HealthCare Pharmaceuticals [Inc, Montville, NJ, USA]. Dicyclohexylcarbodiimide [DCC], Poly ethylene glycol 600 [PEG], Citric acid anhydride, sephadex G-15 fine were purchased from Merck KGaA, [Darmstadt, Germany].

Mouth Epidermal Carcinoma Cells line [KB], Human Embryonic Kidney 293 cell line [HEK 293] and Murine Mammary Adenocarcinoma cells [MMAC] [derived from M05 cell line] were provided by the National Cell Bank of Pasteur Institute of Iran.

#### 3-1 Instrumentation

The Gd<sup>3+</sup> ions were determined by using an inductively coupled plasma atomic emission spectrometer [ICP-AES, JY138 Spectroanalyzer; Horiba JobinYvon, Inc., Edison, NJ]. The zeta-potential of the GALGD was analyzed by Malvern Instruments [Malvern, Worcestershire, UK]. Flowcytometry analyses were carried out by an Epics Altra Hyper sort flow cytometer [Beckman Coulter, Brea, CA, USA] with an air-cooled argon ion laser [488 nm, 15 mW]. This

standard instrument is equipped with two light scatter detectors that measure the forward scatter [FSC] as well as the side scatters. The data were analyzed using the Coulter software.

### 3-2 Animals

The animal experiments were conducted according to relevant national and international guidelines presented by Tehran University of Medical Sciences in correlation with Helsinki's declaration, respectively. All inbred female BALB/c mice [6-8 weeks old, purchased from Iran Pasteur Institute] were kept in large group houses under 12 h dark and light cycles, and given access to food and water ad libitum.

### 3-3 GALGD-G2 Synthesis and Gadobutrol-GALGD-G2 nano-formulations

The ALGD-G2 was synthesized according to the previous reports with slightly modifications.<sup>24,30</sup> By comparing with the previous methods, it is specified that the present procedure has better performance than all other previously described protocols and hasn't the risk of using thionyl chloride (more bio-safety and green chemistry) and decreases the reaction synthesis time, as well.

Briefly, the PEG-600 was selected as the core and reacted with citric acid in the presence of excess amounts of DCC in anhydrous DMF and the dialysis bag was used for the purification. Sephadex G-15 fine<sup>®</sup> [gel filtration chromatography] was used to purify ALGD-G2. Each external 1 mL of eluent buffer for reaction mixture was collected separately in a different tube and its UV-OD/ Iodine TLC spots were monitored to find ALGD-G2.

To formulate Gadobutrol-GALGD-G2, 2 mL of standard gadobutrol [provided from commercially used Gadovist<sup>®</sup>] was added to two different concentrations, 7.26 mL [100 mg dendrimer to provide Gadobutrol+xdendrimer concentration] and 14.5 mL [200 mg dendrimer to provide Gadobutrol+2x dendrimer concentration] of dendrimer and sonicated for at least 15 min. Excess gadobutrol was removed by dialyzing against PBS or alternatively by gel filtration. Iodine TLC spots showed only one spot and indicated that there weren't any starting materials. The Schematic synthesis of GALGD-G2/ Gadobutrol-GALGD-G2 nanoformulation is shown in [Fig. 1].

### 3-4 Cell culture

Mouth Epidermal Carcinoma cell line [KB] and Human Embryonic Kidney cell line [HEK 293] were cultured at 37 °C and 5% CO<sub>2</sub> by using standard cell culture media, containing Dulbecco's Modified Eagle Medium [DMEM]. The cell culture medium was supplemented with 10% fetal bovine serum [FBS] and 1% penicillin – streptomycin.

### 3-5 Apoptosis-Necrosis assay

Apoptosis is considered a different mechanism for certain cell death. The Apoptosis was determined using an Annexin V- propidium iodide staining kit as per the manufacturer recommendations. For cell viability assay, the KB cell line [ $1 \times 10^5$  cells per well] and the HEK [ $1 \times 10^5$  cells per well] were incubated with GALGD-G2 [Gadobutrol+xdenderimer] [5  $\mu$ L], [Gadobutrol+2x denderimer] [5 $\mu$ L], and gadobutrol [5 $\mu$ L] in a 24-well micro-plate, for 24 h with untreated cells as positive control. Each concentration was tested in duplicates [Fig 2, 3].

### 3-6 Nano-formulation intra-cellular uptakes

To detect the intra-cellular uptake of Gadobutrol-GALGD-G2 nanoformulation with two concentrations [Gadobutrol+xdenderimer and Gadobutrol+2x denderimer], the KB cell line was re-plated into 6-well plates at a concentration of  $1 \times 10^5$  cells per well and incubated at 37 °C and 5% CO<sub>2</sub>, for 24 h. GALGD-G2[s] [0.2 and 0.4] and gadobutrol [0.2 and 0.4] were added to each well [1 mL media]. Cells were incubated at 37 °C and 5% CO<sub>2</sub> for 1.5 h, washed twice with PBS [500  $\mu$ L], and then centrifuged at 2500 rpm for 5 min and reconstituted in 100  $\mu$ L of PBS. The intra-cellular uptake of Gd<sup>3+</sup> ions was determined by ICP-AES, quantitatively. The measurements were performed in duplicate and the mean  $\pm$  SD of the results was calculated [Fig4]. The above procedure was performed for Gadovist as well.

### 3-7 Evaluation of Protein Corona

1D SDS PAGE [18%] was employed to probe the protein profiles of the corona coated particles. In this case, 20  $\mu$ L of protein loading buffer was added to 80  $\mu$ L of the hard corona coated NPs; after boiling for 4 min, 15  $\mu$ L of each sample was loaded in each well. Finally, the silver staining was performed to detect protein bands. As temperature has crucial effect on the composition of protein corona, tight control was implemented on fixing the incubation temperature at 37°C.<sup>30, 31</sup>

## 4- MR measurement and Stability Studies

The relaxation times of Gadobutrol-GALGD-G2 nanoformulation and Gadovist were also measured at different concentrations by using different spin echo and gradient echo protocols in 1.5 Tesla MRI with a head coil. Multiple spin echo protocols were used for T<sub>2</sub> measurement. In total, 32 echoes were obtained with an echo spacing of 2 ms. The first echo time [TE] was 22 with TR of 3000 ms, Matrix=256 $\times$ 256; slice thickness=1.5 mm, non-averaged. A FLASH protocol was used to calculate T<sub>1</sub> maps. Replication times of TR= 32, 50, 100, 200, 400, 600, 1000, 2000 and 3000 ms; TE was 12 ms; matrix=256 $\times$ 256; slice thickness=1.5 mm, and non-averaged. For quantitative analysis, the MRI images were analyzed by DICOM software version 1.3.0.5. [MEDAV GmbH Company]. The above similar procedure was performed 3 and 6 months after formulation for investigation of any unwanted occurred instabilities.

#### 4-1 *In vivo* MRI preparation

An adult mouse [provided by Pasteur Institute of Iran and treated based on the declaration of Helsinki] subjected to suffer from cancer and weighting about 20 g, was used for *in Vivo* study. The mouse 4T1 breast cancer cells trypsinized and re-suspended in 10-fold excess culture medium. After centrifugation, the cells were re-suspended in serum-free medium, and  $1 \times 10^6$  cells injected subcutaneously in a final volume of 0.1 mL using a 21-gauge needle in the left flank of BALB/c mice under ketamine and xylazine [10 mg/kg, i.p] anesthesia. Tumor growth was visible after 4-6 weeks of injection. The tumor images were obtained, 5 min after tail vein injection of 0.2 mL/kg/B.W, of Gadobutrol-GALGD-G2 nanoformulation~ (each mL contained 12 mg gadobutrol and Gadovist) and ~ (each mL contained 120 mg gadobutrol), using MRI scanner.<sup>18</sup>

#### 5- Pathological Findings

One week after imaging, all the injected animals were sacrificed ethically and Kidney tissues of healthy and treated animals were collected in formalin and the by preparation of pathological stained lam [H& E staining] all the subjected tissues were evaluated for examining any pathological defects.

#### 6- Statistical Analysis

Multi group comparisons were carried out by one-away ANOVA and its post hoc TUKEY test. Statistical significance for cell toxicity was set at  $P < 0.05$ . Results are expressed as the data mean  $\pm$  SD.

#### 7- CONCLUSION

The large and linear transverse relaxation of  $Gd^{3+}$ -DO3A-butrol -GALGD-G2 nanoformulation provides such contrast agent with good sensitivity and low pathotoxicological effects for cellular and molecular imaging in 1.5 Tesla MRI. Future experiments might be desirable to further study the cellular uptake mechanisms of  $Gd[III]$ -DO3A-butrol -GALGD-G2 nanoformulation and its subcellular localization. These findings provide helpful insights in designing efficient contrast agents for nano-carriers delivery to cancerous tissues.

#### ACKNOWLEDGEMENTS

We deeply appreciate all academic staff as well as the technicians for their kindly support during the course of experiments.

#### Disclosure

This research forms the major part of M.S thesis of Biochemistry by Elham Mohammadi in Mazandaran University of Medical Science. All authors declare that they have no conflicts of interest associated with this work.

### Bibliographic references and notes

1. Moscow, J.; Cowan, K.. 23rd ed; Cecil Medicine, Saunders Elsevier Publications: Philadelphia, 2007.
2. Raymond, K. N.; Pierre, V.C.. *Bioconjug. chem.* 2005, 16[1], 3-8.
3. Mohammadi, D. T.; Amanlou, M.; Ghalandarlaki, N.; Mehravi, B.; Shafiee Ardestani, M.; Yaghmaei, P.. *ISRN pharmaceuticals*. 2013.
4. Anand, P.; Kunnumakara, A. B.; Sundaram, C.; Harikumar, K. B.; Tharakan, S. T.; Lai, O. S.; Sung, B.; Aggarwal, B. B. *Pharmaceutical research*. 2008, 25 [9], 2097-2116.
5. Weishaupt, D.; Köchli, V.D.; Marincek, B. Springer, 2003
6. Koenig, S.; Brown, R.; Gupta, R. CRC Press: Boca Raton, FL, 1987.
7. Mirzaei, M.; Mohagheghi, M.; Shahbazi-Gahrouei, D.; Khatami, A. *J. Biomater. Nanobiotechnol.* 2013, 4[1], 22-29.
8. Weinmann, H. J.; Brasch, R. C.; Press, W. R.; Wesbey, G. E. *AJR. Am. J. Roentgenol.* 1984, 142(3), 619-624.
9. Zhou, Z.; Lu, Z. R. *Rev. Nanomed. Nanobiotechnol.* 2013, 5 (1), 1-18.
10. Westbrook, C. John Wiley & Sons, 2013.
11. Allen, M. J.; Meade, T. J. *J. Biol. Inorg. Chem.* 2003, 8 (7), 746-750.
12. Bhorade, R.; Weissleder, R.; Nakakoshi, T.; Moore, A.; Tung, C. H. *Bioconjug. chem.* 2000, 11 [3], 301-305.
13. Wunderbaldinger, P.; Josephson, L.; Weissleder, R. *Bioconjug. chem.* 2002, 13 (2), 264-268.
14. Lewin, M.; Carlesso, N.; Tung, C. H.; Tang, X. W.; Cory, D.; Scadden, D. T.; Weissleder, R. *Nature biotechnology*. 2000, 18 (4), 410-414.
15. Mehravi, B.; Ahmadi, M.; Amanlou, M.; Mostaar, A.; Ardestani M. S.; Ghalandarlaki, N. *Int. J. Nanomedicine*. 2013, 8, 3209.
16. Mehravi, B.; Ahmadi, M.; Amanlou, M.; Mostaar, A.; Ardestani, M. S.; Ghalandarlaki, N. *Int. J. Nanomedicine*. 2013, 8, 3383. Langereis S, Lussanet Q, Meijer GEW, Beets-Tan RGH, Griffioen AW, Engelshoven JMAV, Backes WH. *NMR Biomed.* 2006;19:133-141
17. Dodd, C. H.; Hsu, H. C.; Chu, W. J.; Yang, P.; Zhang, H. G.; Mountz, J. D.; Zinn, K.; Forder, J.; Josephson, L.; Weissleder, R. *J. Immunol. Methods*. 2001, 256 (1), 89-105.
18. Mehravi, B.; Ardestani, M. S.; Damercheli, M.; Soltanghoreae, H.; Ghanaldarlaki, N.; Alizadeh, A. M.; Oghabian, M. A.; Shirazi, M. S.; Mahernia, S.; Amanlou, M. *Mol. Imaging Biol.* 2014, 1-10.
19. Mirzaei, M.; Mohagheghi, M.; Shahbazi-Gahrouei, D.; Khatami, A. *Journal of Nanomedicine & Nanotechnology*. 2012, 3 (7).
20. Wiener, E.; Brechbiel, M.; Brothers, H.; Magin, R.; Gansow, O.; Tomalia, D.; Lauterbur, P. *Magn. Reson. Med.* 1994, 31 (1), 1-8.
21. Perazella, M. A. *Clin. J. Am. Soc. Nephrol.* 2009, 4 (2), 461-469.
22. Botta, M.; Tei, L. *Eur. J. Inorg. Chem.* 2012, (12), 1945-1960.
23. Daldrup, H.; Shames, D. M.; Wendland, M.; Okuhata, Y.; Link, T. M.; Rosenau, W.; Lu, Y.; Brasch, R. C. *AJR. Am. J. Roentgenol.* 1998, 171 (4), 941-949.
24. Haririan, I.; Alavidjeh, M. S.; Khorramizadeh, M. R.; Ardestani, M. S.; Ghane, Z. Z.; Namazi, H. *Int. J. Nanomedicine*. 2010, 5, 63.
25. Alavidjeh, M. S.; Haririan, I.; Khorramizadeh, M. R.; Ghane, Z. Z.; Ardestani, M. S.; Namazi, H. *J. Mater. Sci. Mater. Med.* 2010, 21(4), 1121-1133.
26. Klajnert, B.; Bryszewska, M. *Acta Biochim. Pol.* 2000, 48 (1), 199-208.
27. Antoni, P.; Hed, Y.; Nordberg, A.; Nyström, D.; Von Holst, H.; Hult, A.; Malkoch, M. *Angew. Chem. Int. Ed. Engl.* 2009, 121 [12], 2160-2164.

28. Jain, K.; Kesharwani, P.; Gupta, U.; Jain, N. *Int. J. Pharm.* 2010, 394 [1], 122-142.
29. D'Emanuele, A.; Attwood, D.. *Adv. Drug Deliv. Rev.* 2005, 57 [15], 2147-2162.
30. Mahmoudi, M.; Lohse, S. E.; Murphy, C. J.; Fathizadeh, A.; Montazeri, A.; Suslick, K.S. *Nano Letters*. 2014, 14 [1], 6-12.
31. Mahmoudi, M.; Abdelmonem, A. M.; Behzadi, S.; Clement J. H.; Dutz, S.; Ejtehadi, M. R.; Hartmann, R.; Kantner, K. *ACS Nano*. 2013, 7 [8], 6555.
32. Mahmoudi, M.; Lynch, I.; Ejtehadi, M. R.; Monopoli, M.P.; Bombelli, F. B.; Laurent, S. [2011] *Chemical Reviews*. 2011, 111, 5610-5637.
33. Mirshafiee, V.; Mahmoudi, M.; Lou, K.; Cheng, J.; Kraf, M. L. *Chem Communications*. 2013, 49[25], 2557-9.
34. Ghavami, M.; Saffar, S.; Abd Emamy, B.; Peirovi, A.; Shokrgozar, M. A.; Serpooshan, V.; Mahmoudi M. *RSC Advances*. 2013, 3, 1119-1126.
35. Mirzaei, M.; Mohagheghi, M.; Shahbazi-Gahrouei, D. *J. Biomat. Nanobiotech*. 2013, 4 [1].
36. Abu-Rmaileh, R.; Attwood, D.; Emanuele, A. Dendrimers in cancer therapy. *Drug Del. Sys. Sci.* 2003, 3:65-70.
37. Tang, A. M.; Ananta, J. S.; Zhao, H.; Cisneros, B. T.; Lam, E. Y.; Wong, S. T.; Wilson L. J.; Wong, K. K. *Contrast Media Mol. Imaging*. 2011, 6 [2], 93-99.
38. Ghalandarlaki N, Mohammadi TD, Agha Babaei R, Tabasi MA, Keyhanvar P, Mehravi B, Yaghmaei P, Cohan RA, Ardestani MS. *Drug Res (Stuttg)*. 2014;64(2):57-65.

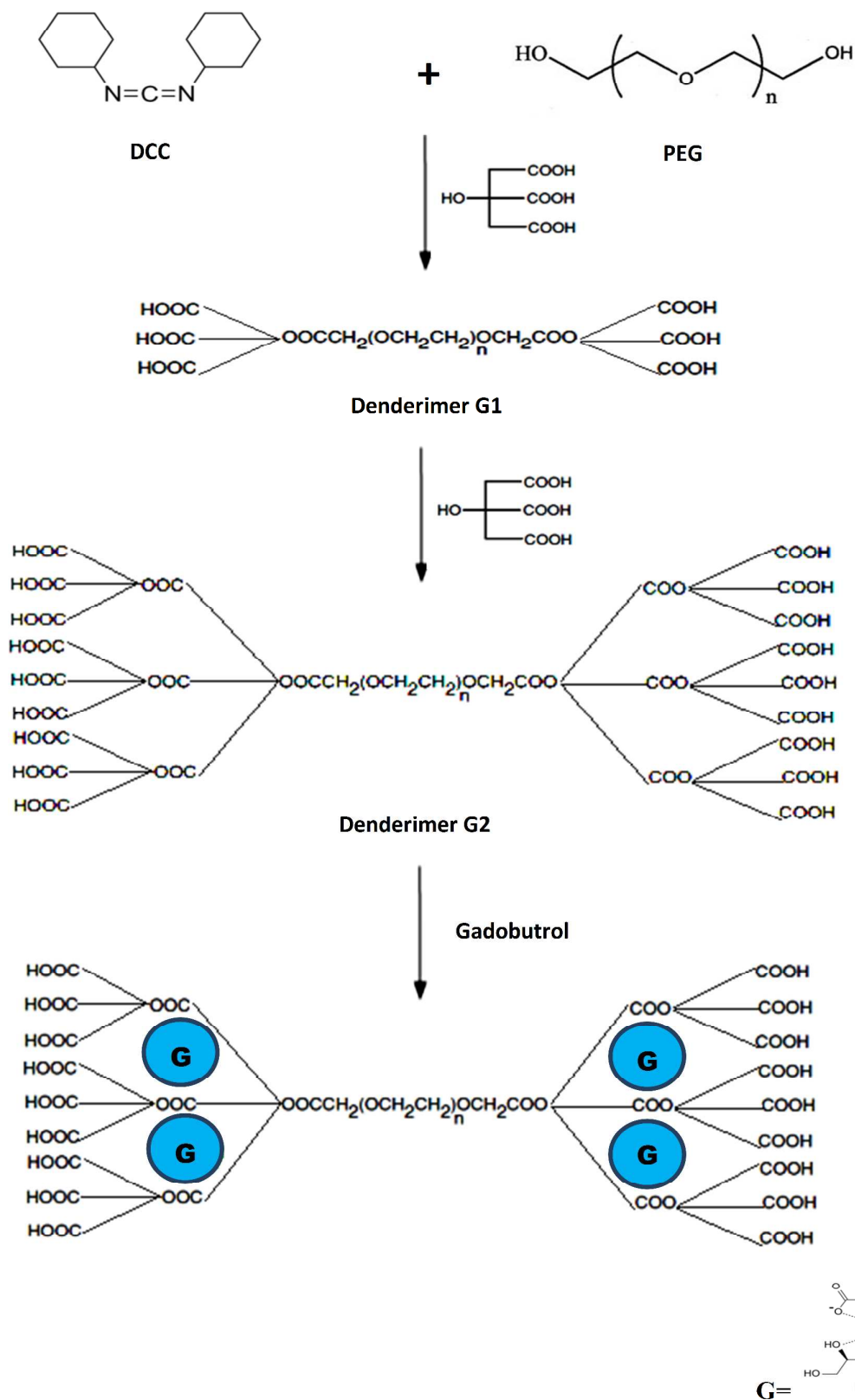


**Figure 1.** Process of preparing Gadobutrol-GALGD-G2.

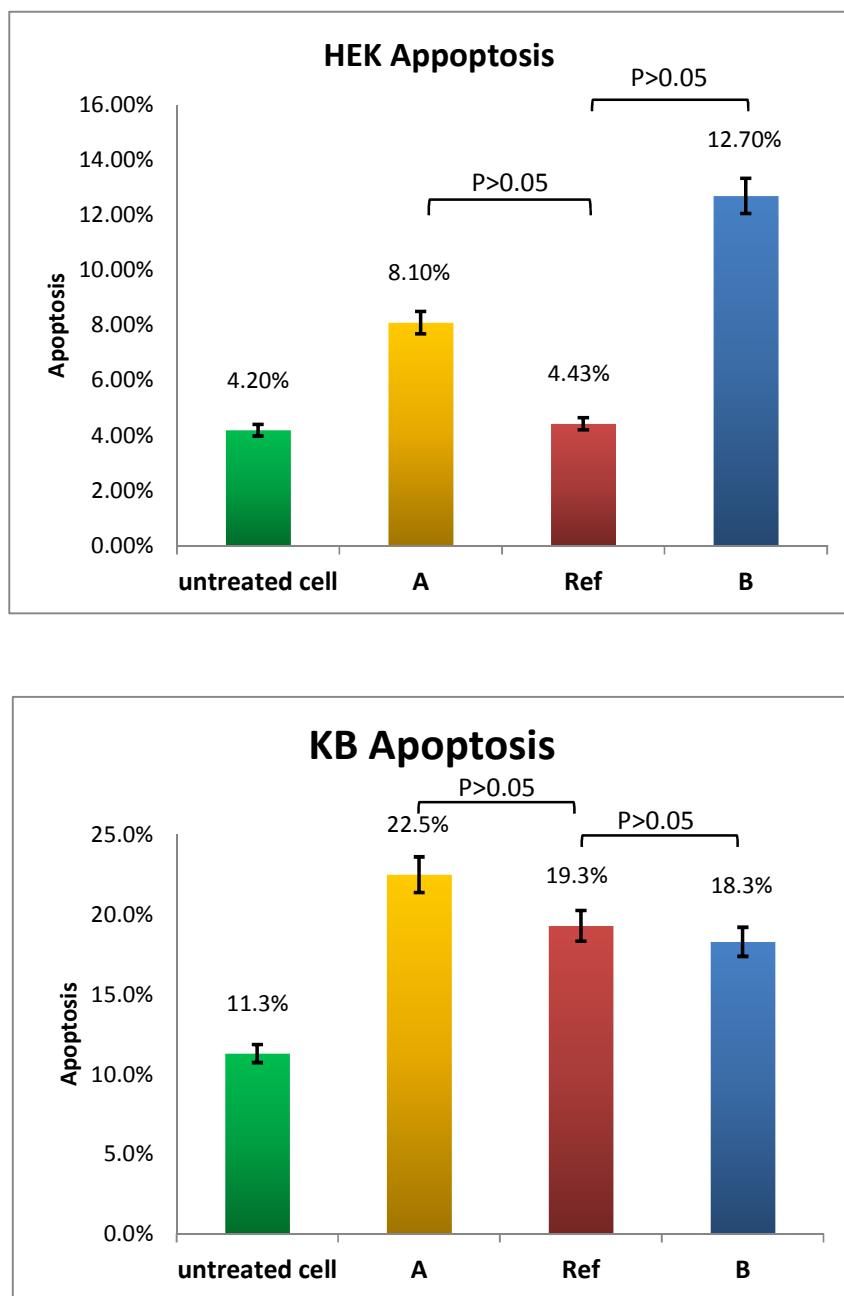


**Figure 2.** Apoptosis percentage of treated KB cells and HEK cell with GALGD-G2 [ $P > 0.05$ ].

**Abbreviations:** GALGD, Anionic Linear Globular Dendrimer G2 conjugated with gadobutrol; KB, Mouth Epidermal Carcinoma Cells line. HEK, Human Embryonic Kidney 293 cells

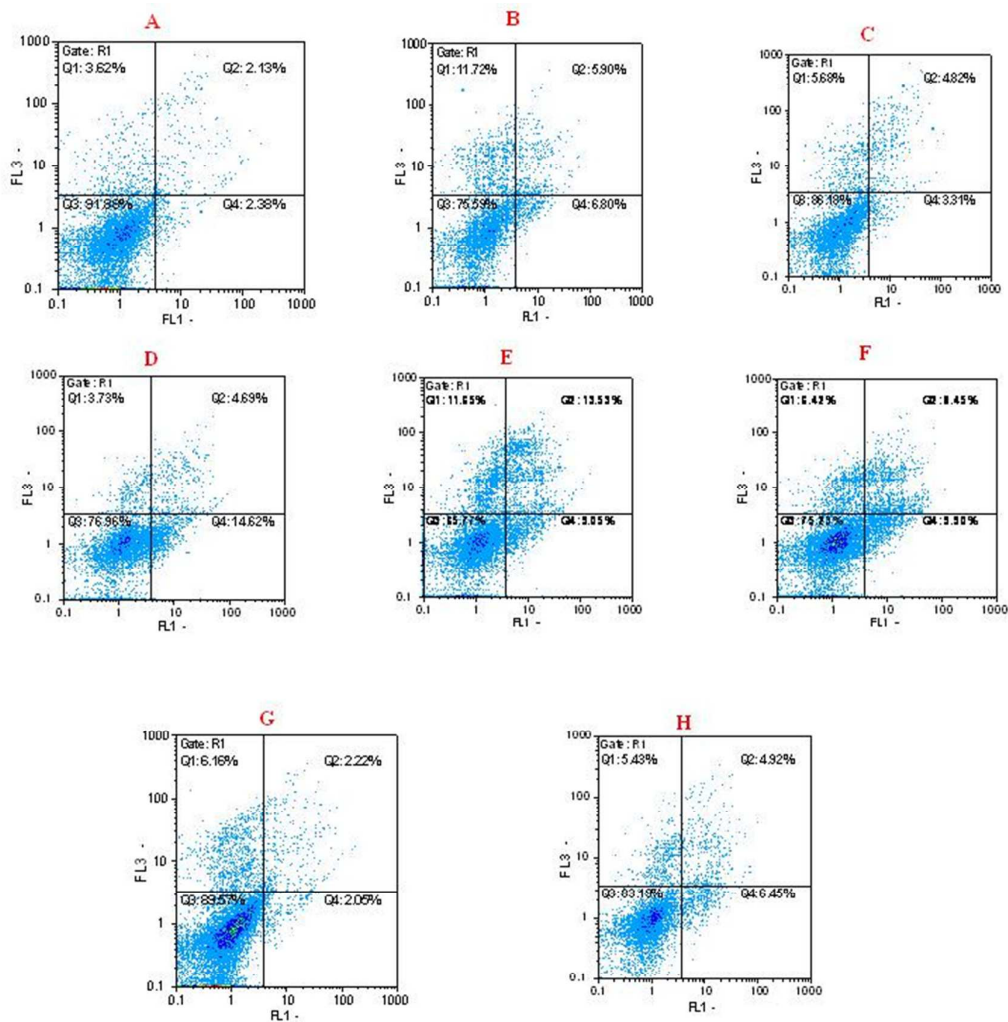


**Fig3.** Cellular apoptosis/ necrosis percentage comparison data obtained by flowcytometry in two normal HEK and cancerous KB cell line].

Respectively HEK and KB cell line treatment with gadobutrol [5  $\mu$ g-A, B], Gadobutrol+x denderimer [5  $\mu$ g C, D], Gadobutrol+2x denderimer [5  $\mu$ g, E, F], and HEK293 cells [G] stained, KB cells [H] stained with no treatment.

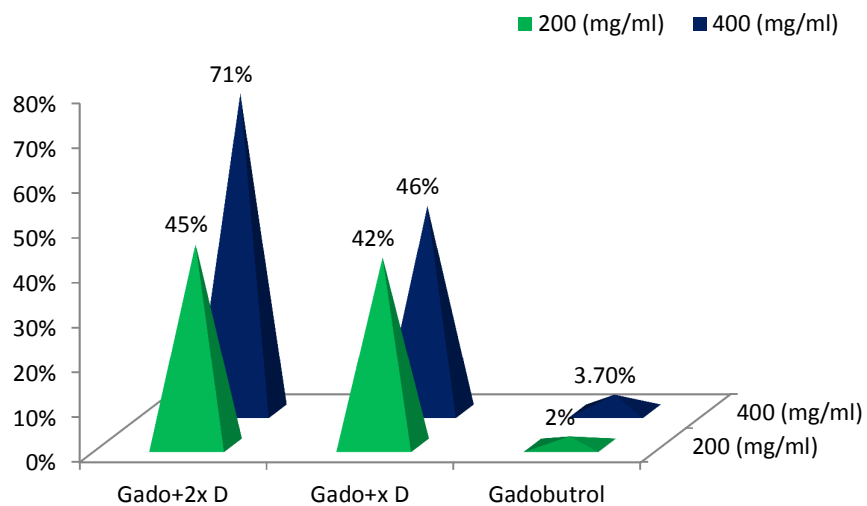


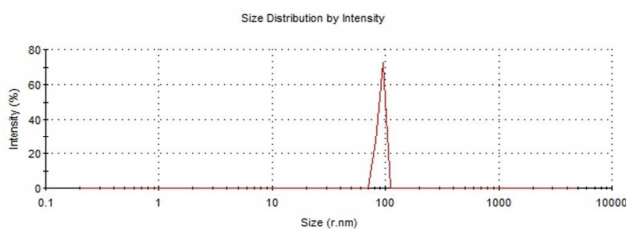
**Figure 4.** Cell uptake assay of GALGD-G2: Results indicated the dendrimer effect on intracellular uptake [ $P < 0.05$ ].

**Abbreviations:** GALGD, Anionic Linear Globular Dendrimer G1 conjugated with gadobutrol; KB, Mouth Epidermal Carcinoma Cells line.

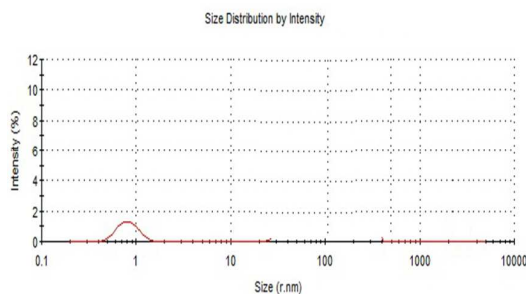
Zeta potential [mV] of Gadobutrol	Zeta potential [mV] of GALGD2[G+2XD]	Zeta potential [mV] of GALGD2[G+XD]
-5.50	-18.5	-12.7

**Table1.** Zeta potential of Gadobutrol and GALGD2. The zeta potential of the drug reduced after attaching dendrimer.

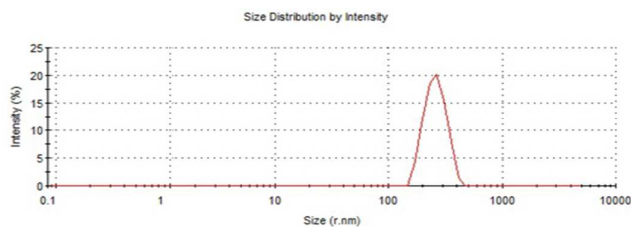
A



B



C



D

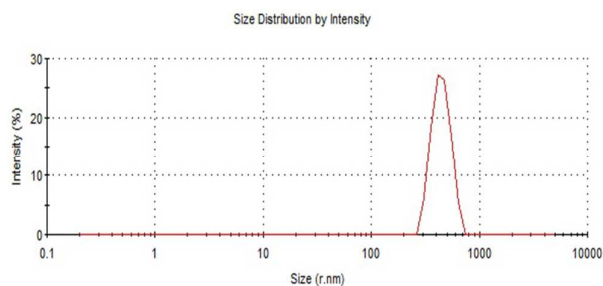
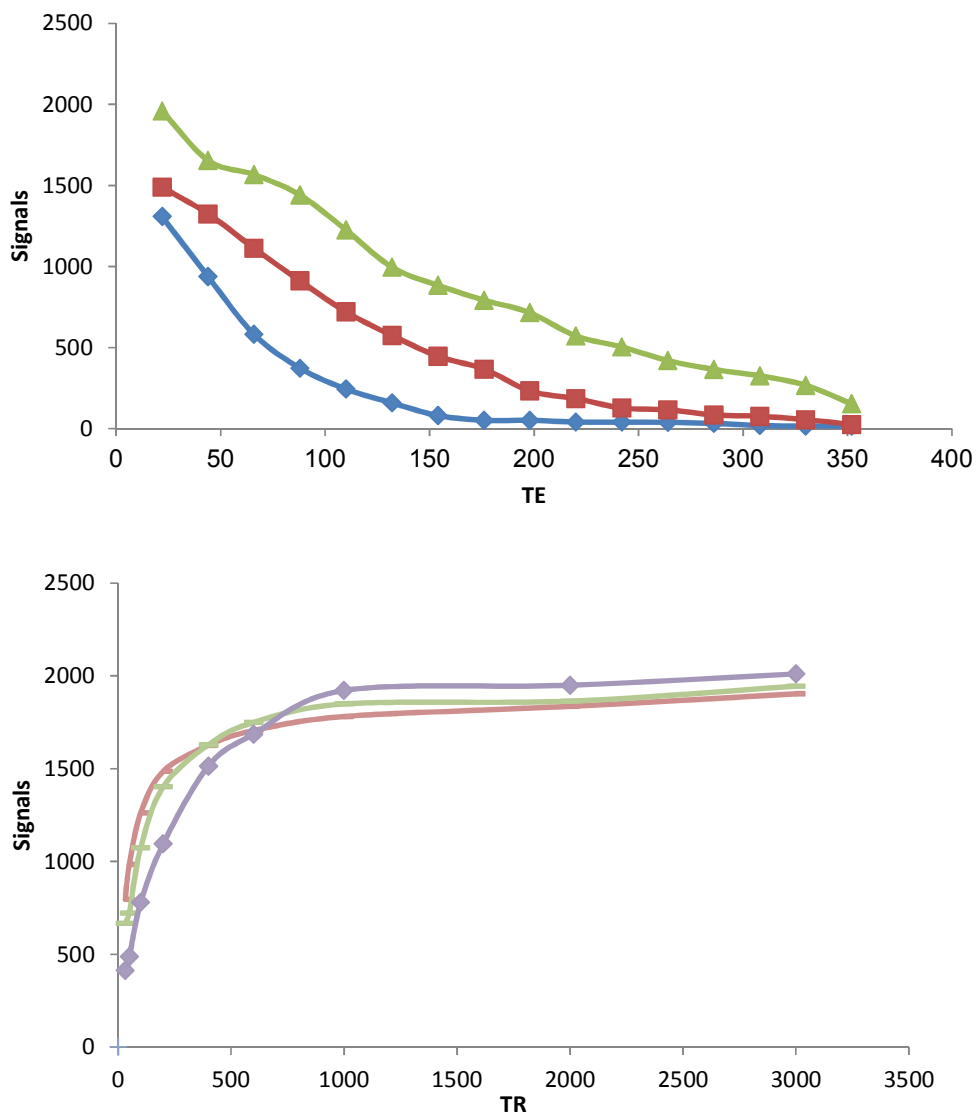
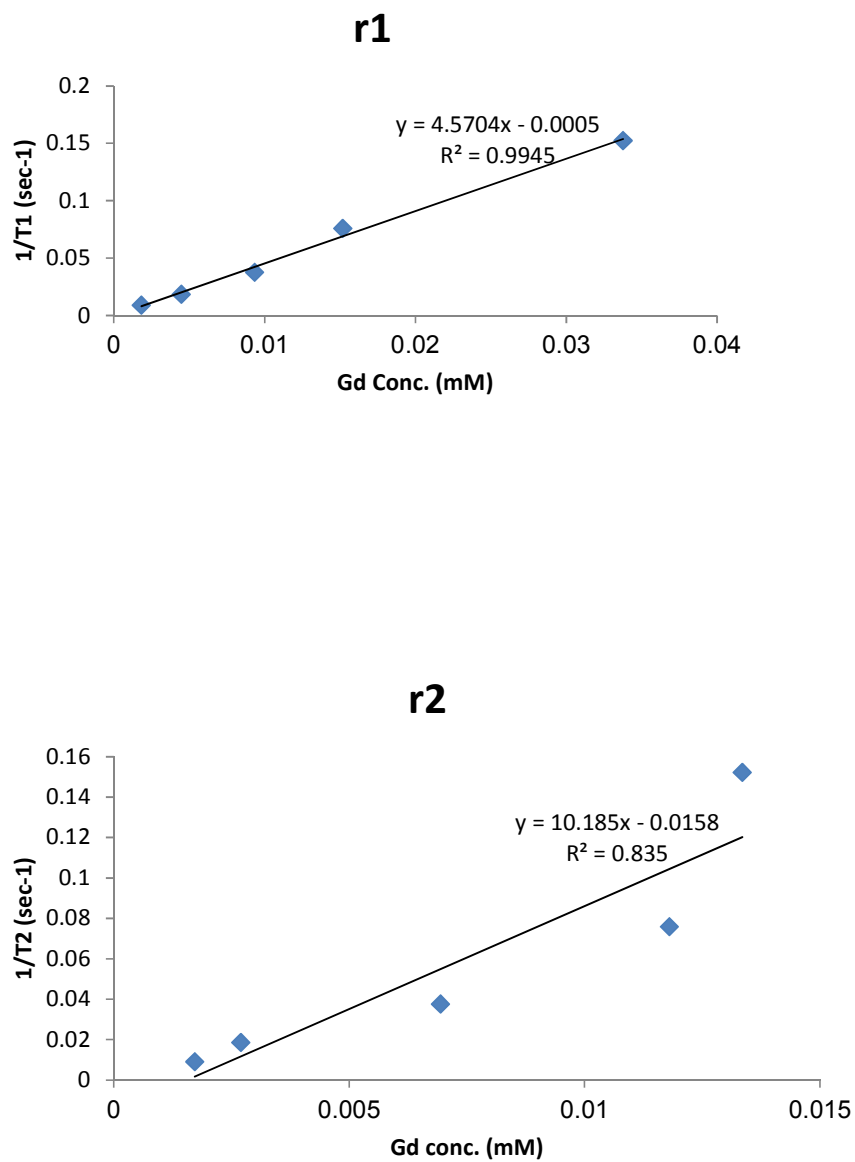


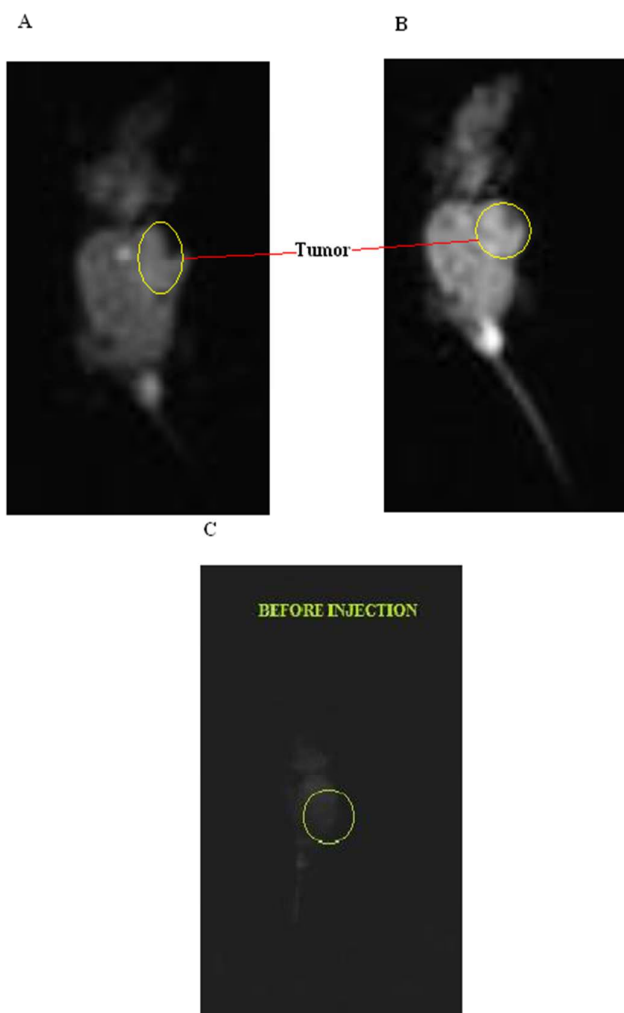
Fig 5. Zeta sizer reported a significant increase in size of the dendrimer after attaching gadobutrol incorporation. Original Size distribution of Dendrimer-G2 [A], Gadobutrol [B] and Gadobutrol nano-formulation x [C] and Gadobutrol nano-formulation 2x [D] was depicted respectively.



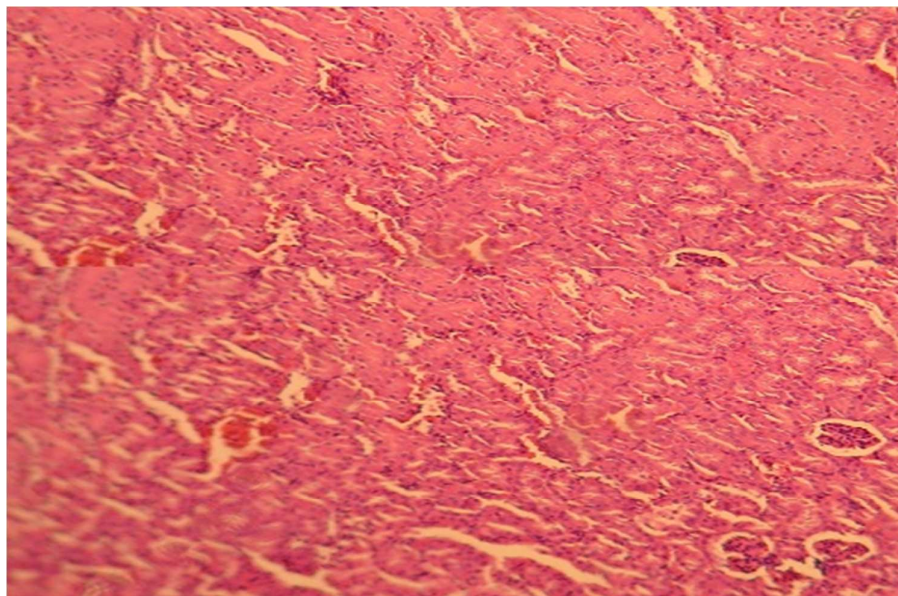
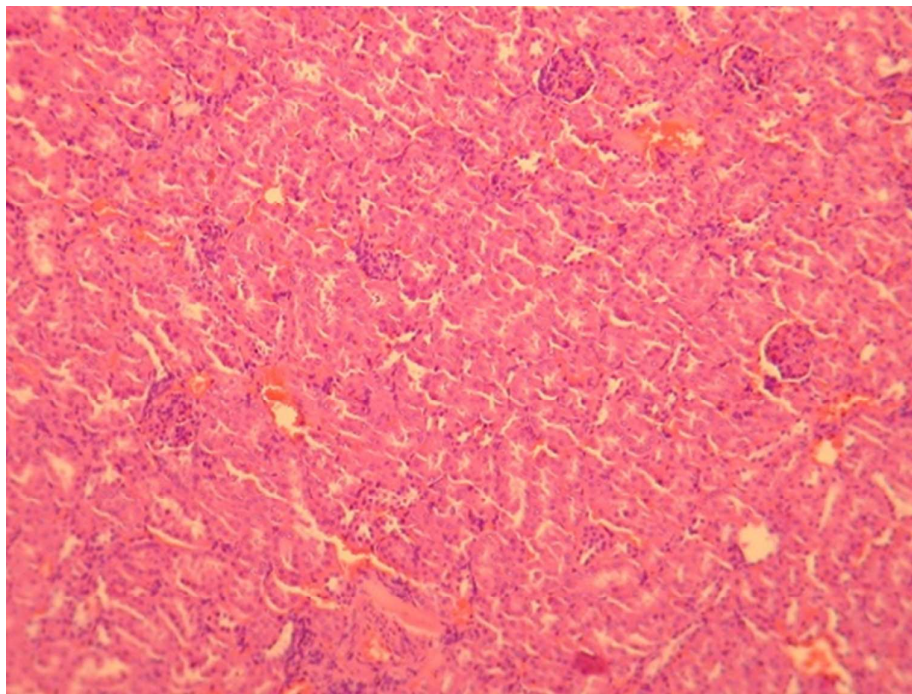
**Figure 6.**  $T_1$  and  $T_2$  data based on spin echo and gradient echo protocols



**Figure 7.** The relaxivity curves of GALGD-G2: A]  $r_1$  relaxivity, B]  $r_2$  relaxivity



**Figure 8:** MR images [C] pre-injection and [B] 5 minutes post-injection. Tumor growth was visible 4–5 weeks post injection. This result shows the ability of GALGD-G2 in enhancing the T<sub>1</sub>-weighted images. Additionally, single Gadobutrol injection did not provide any tumor enhancement [A].  
**Abbreviations:** MRI, magnetic resonance imaging; GALGD-G2, anionic linear globular denderimer G2 conjugated to gadobutrol; KB, Mouth Epidermal Carcinoma Cells line cancer cells.

**A****B**

**Fig 9.** Pathological findings of kidney H & E staining showed not any significant defects resulted in the administration of 0.2mmole/Kg Dendrimer-Gadobutrol [Control A and Treated B]

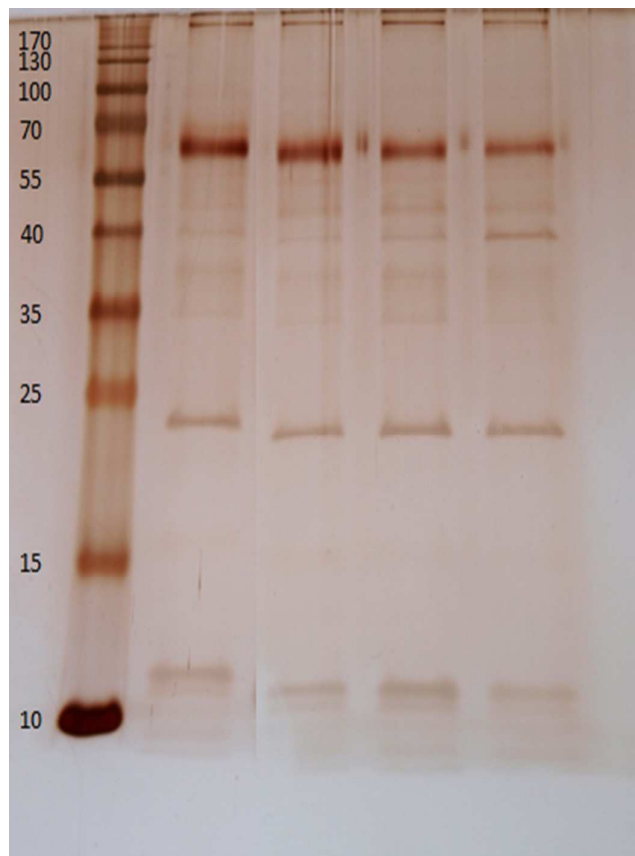


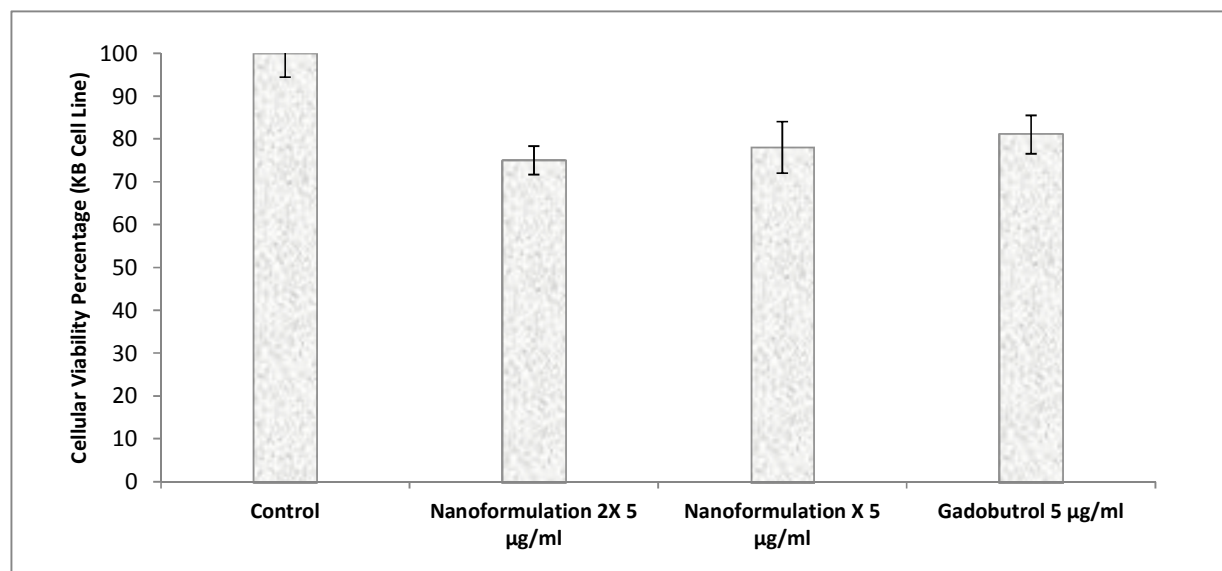
Fig 10. SDS-PAGE of protein profile obtained from various particles [Dendrimers G1, G2 and Dendrimer G2-Gadobutrol [dosages X and 2X]] complexes free from excess plasma following 1 h incubation at a temperature of 37°C. The molecular weights of the proteins in the standard ladder are shown on the left as reference.

## Supplementary Materials:

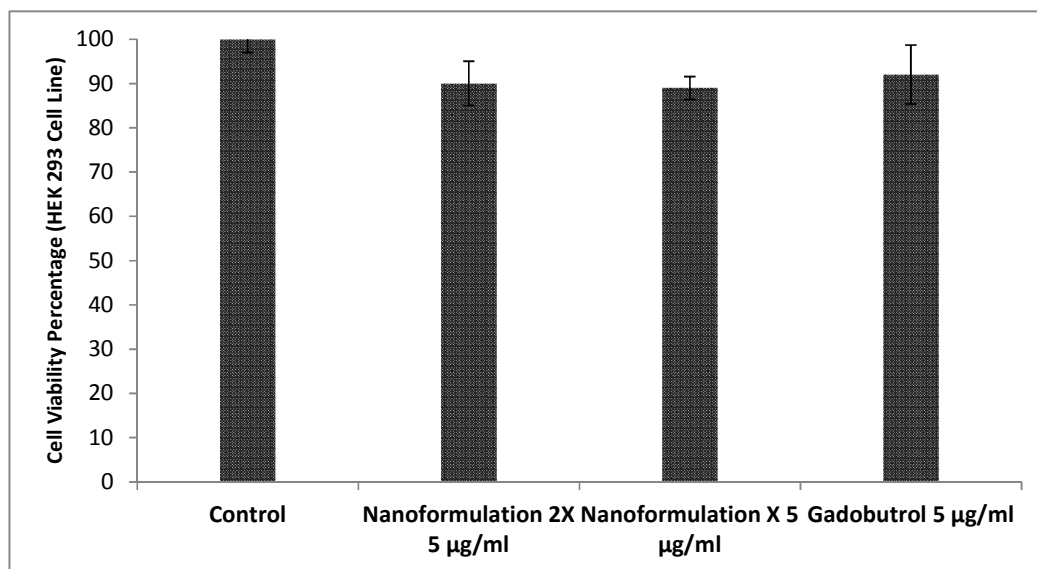
### Cellular Toxicity Assay (MTT)

Based on the previously published literature<sup>14-17</sup> both tumor (MCF-7) and normal (HEK-293) cells lines, provided from National Cell Bank of Pasteur Institute of Iran, were cultured and exposed to the same concentration (5 $\mu$ g/ml) of the different nano-formulated contrast agent and gadobutrol for a period of 24 hrs and OD was obtained from ELISA reader at 570 nm respectively. The MCF-7 cellular exposures showed a mild significant  $p < 0.05$  cellular toxicity for Nano-formulation 2X as well as a not significant cellular toxicity  $p > 0.05$  for those of Nano-formulation X and gadobutrol. Furthermore, not any HEK-293 cellular toxicity was observed from the nano-formulations and gadobutrol exposures. (See original data at S-1<sub>a-b</sub>) Briefly, gadobutrol was shown to be safe and insert both normal and cancer cell line but the gadobutrol nanoformulation was found safe on normal human kidney cell line (as a major toxicity target of gadolinium based contrast agent) and toxic on cancer cell lines.

**S-1<sub>a</sub>:** Results of the same concentration (5 $\mu$ g/ml) of the different nano-formulated contrast agent and gadobutrol for a period of 24 hrs on MCF-7 cell lines.



S-1<sub>b</sub>: Results of the same concentration (5 $\mu$ g/ml) of the different nano-formulated contrast agent and gadobutrol for a period of 24 hrs on MCF-7 cell lines. S-1<sub>a</sub>: Results of the same concentration (5 $\mu$ g/ml) of the different nano-formulated contrast agent and gadobutrol for a period of 24 hrs on HEK-293 cell lines.

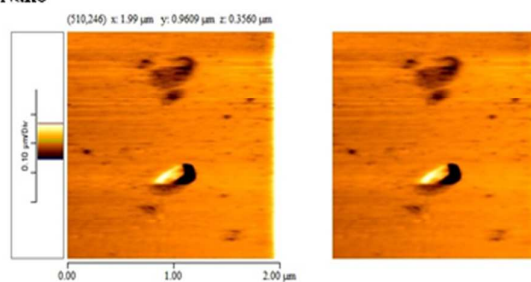


## AFM Imaging

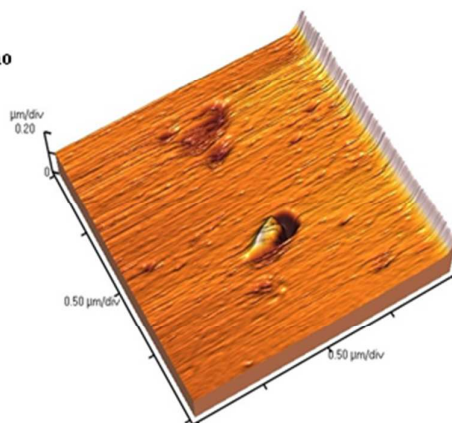
For morphology investigations of the proposed nano-formulations X and 2X Atomic Force Microscopy were employed and two and three dimensional images were obtained as demonstrated in S-2<sub>a</sub> and S-2<sub>b</sub>.

### S-2<sub>a</sub>: 2D and 3D AFM images of nanoformulation X.

2D-X Nano

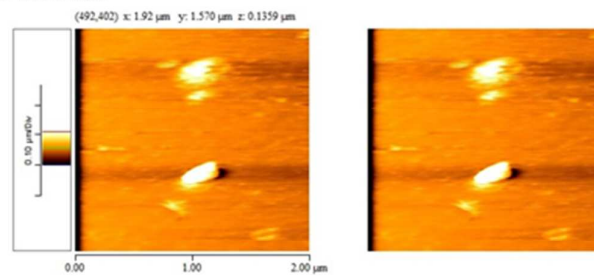


3D-X Nano

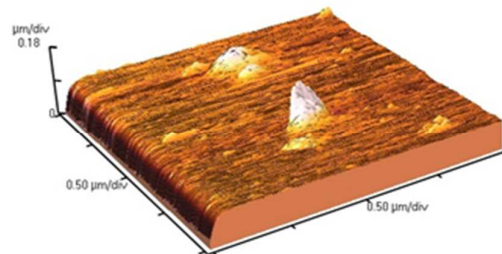


S-2<sub>b</sub>: 2D and 3D AFM images of nanoformulation 2X.

2D-2X Nano



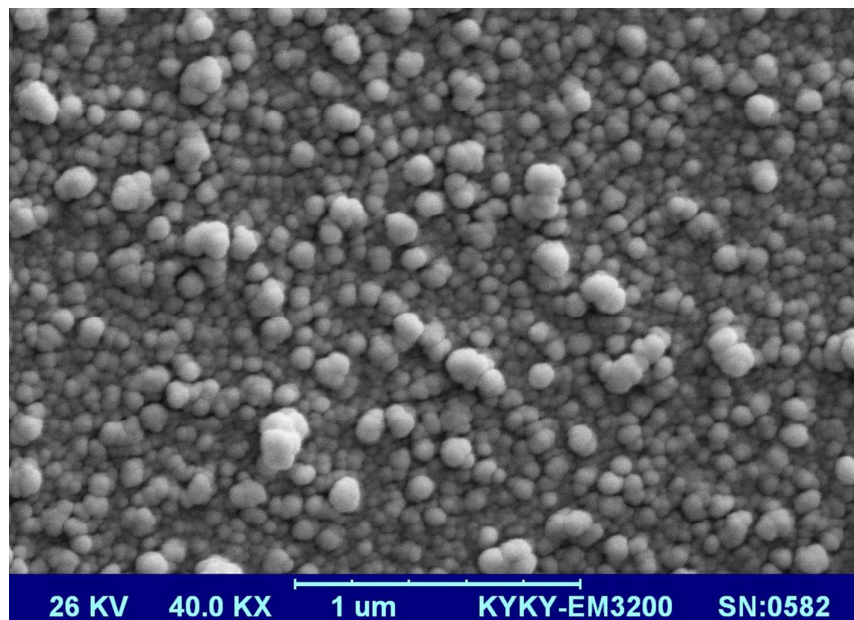
3D-2X Nano



## SEM Imaging

For more morphology investigations of the proposed nano-formulations X and 2X sizes, Single Electron Microscopy were used and images were obtained as demonstrated in S-3<sub>a</sub> and S-3<sub>b</sub>. Before preparation of imaging samples the formulations were rigorously sonicated to avoid any unwanted nanoparticle's aggregations. According to the results sizes obtained at a lower ranged (<200 nm) than observed by AFM or Zetasizer's data.

**S-3<sub>a</sub>: SEM image of X nano-formulation**



**S-3<sub>b</sub>: SEM image of 2X nano-formulation**

